

Inside this issue

- 1 **Focal Point:** TissueGnostics Tissue Cytometric System
- 2 **New equipment and services:** Immunogold EM, Platinum replica EM, Phosphoimager
- 4 **Technical Spectra:** Deconvolution vs. Confocal

FOCAL POINT

TissueGnostics Tissue Cytometry System

The facility has been selected to be the U.S. reference site for the powerful Cell Analysis System from TissueGnostics, Inc. (Vienna, Austria), which is now permanently housed in Morton 2-664. This system was purchased with the generous matching fund from the Robert H. Lurie Comprehensive Cancer Center.

The TissueGnostics Cell Analysis System provides several functions that are vitally important for researchers who study tissue specimens and for those who need to perform cellular and tissue cytometric analysis.

Equipped with a monochrome CCD camera and a color

camera, the TissueGnostics system is capable of acquiring both fluorescent and brightfield images, thus greatly expanding users' repertoire in performing the type of cytometric analyses of their choice.

Through its automated sample scanning function, the system can automatically scan up to eight slides placed on the stage, and perform tissue-stitching functions to create a large overview of the entire sample without losing details at high resolution, as indicated in figure 1. This feature thus allows users to scan their slides in a high throughput manner and

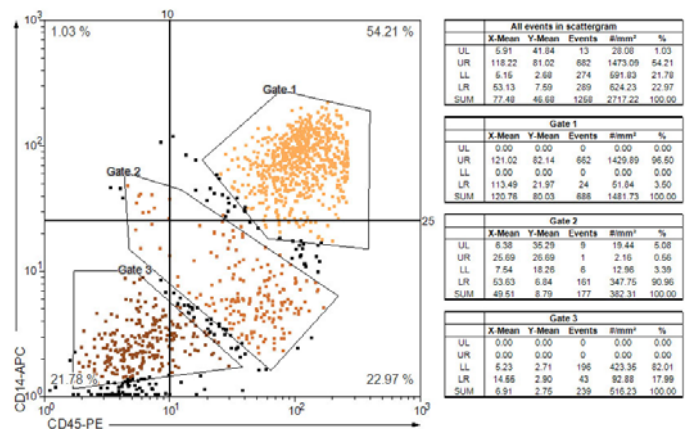


Figure 2. Each cellular "event" will be plotted in a scattergram by the TissueGnostics software. Users can easily define any combination of X- and Y-axis parameters to directly compare any combination of phenotype of the cells in the specimen. The software also allows users to gate any population of cells and immediately obtain rigorous statistical analyses. More importantly, users can pinpoint the actual "gated" population of cells within the specimen.

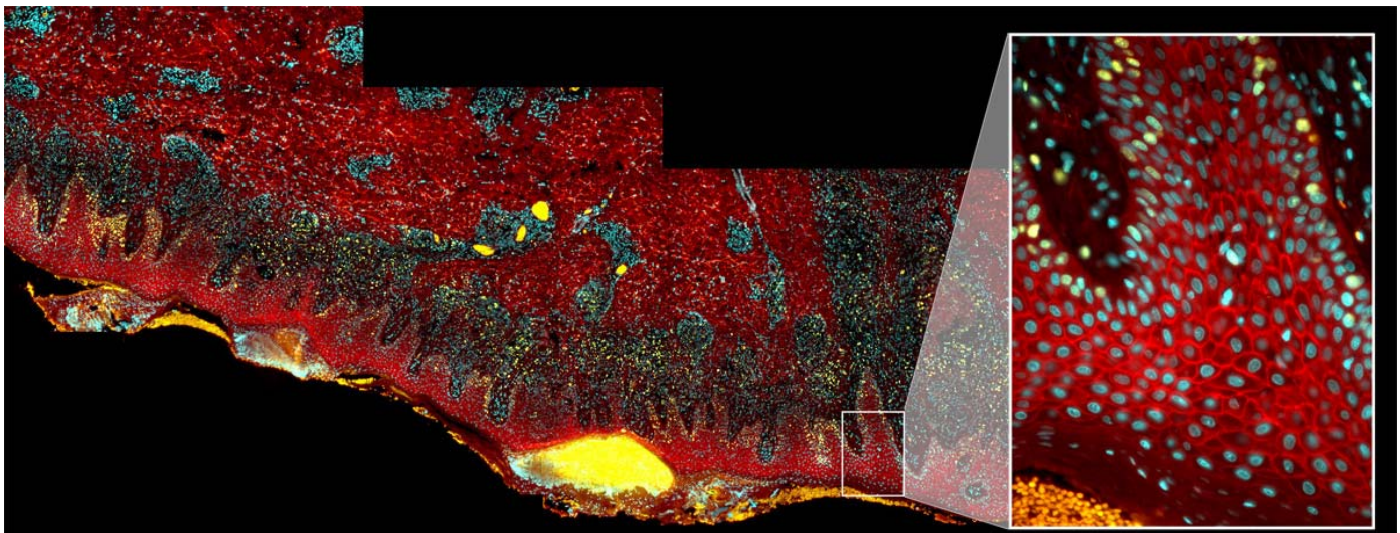


Figure 1 Tissue-stitching function of Tissuegnostics Cell Analysis System creates "virtual slides" that contains large overview of tissue specimens without losing accuracy in details.

store the specimens digitally for immediate and future analysis. Both fluorescence and brightfield imaging can be performed on the Cell Analysis System.

Once the region of interest has been scanned, and the montaged "virtual slide" has been obtained, the image analysis software will automatically detect individual cells, and each cellular "event" will be represented in a flow-cytometry-like scattergram (see figure 2).

The scattergram functions precisely like a flow cytometry dotplot wherein one can gate any subpopulation of cells based on any combination of distributions of fluorescence intensity and size. Statistical data will be instantly displayed by the TissueGnostics system for each gated quadrant. The TissueGnostics system is also capable of bi-directional data viewing. A gated population of cells within the scattergram can be easily traced back to their actual histological location in the specimen, as can be seen by the interactive display attached below in Figure 3.

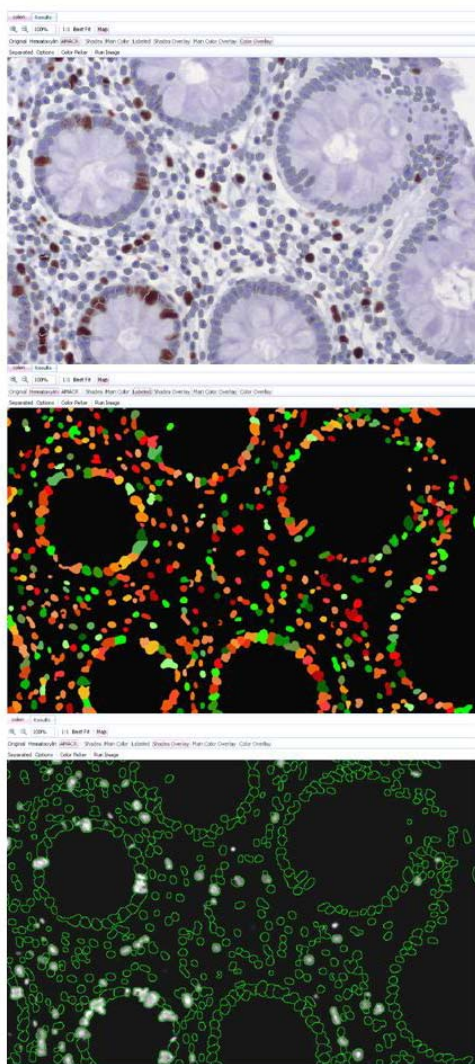


Figure 3 Cell recognition capability of the HistorQuest software module of the TissueGnostics system. The top panel shows the color-separated image of an H&E-stained tissue sample. The automatic color separation can be easily defined by the users. The middle panel shows each individual cells recognized by the software through morphometric analysis. The third panel shows cells with specific staining pattern in the context of total cell count.

By clicking on any given cell in the image, users can also directly trace its phenotypic profile back to the scattergram. The free hand gating function also allows user to perform unbiased statistical analysis based on the scattergrams rather than on the images, as shown in Figure 2.

NEW EQUIPMENT AND SERVICES

Immunogold Electron Microscopy

Immunocytochemistry can be combined with electron microscopy to study the detailed microarchitecture of tissues or cells. This technique allows the detection of specific proteins in ultrathin tissue sections. Antibodies labelled with heavy metal particles (e.g. gold) can be directly visualised using transmission electron microscopy.

The Cell Imaging Facility is now offering immunogold electron microscopy service. Immunogold technique can be applied to tissue, *in vitro* cultured cells, as well as purified proteins (figure 4).

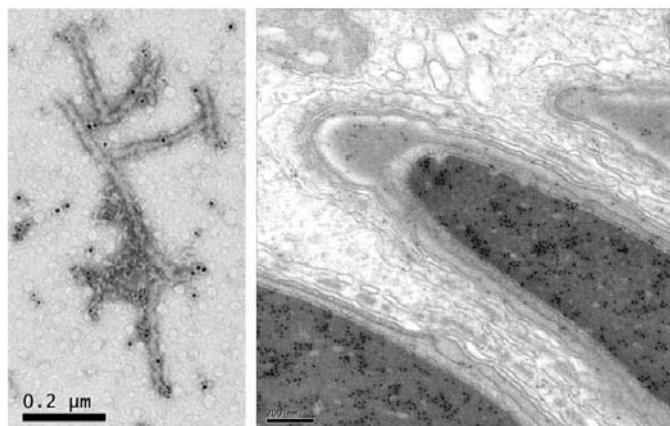


Figure 4. **A.** Immunogold localization (with 6nm and 10nm gold particles) performed on purified protein preparation. (Picture Courtesy of Sara Kleinschmidt and Dr. Adriana Ferraira). **B.** Immunogold localization of Pum2 protein in mouse testis section. Staining was detected in in the nucleus and membrane of elongating spermatids (Picture Courtesy of Dr. Chirag Shah and Dr. Eugene Xu)

There are many factors that govern the course and specific details of an experiment. Unfortunately trial and error play a large role in the eventual outcome of an immunocytochemistry experiment.

One of the major elements that can significantly alter the outcome of immunogold EM is fixation condition. More so than in light microscopy, the antigenic determinant is easily altered or masked during fixation and sample preparation for EM. It is clear that antigens do not respond uniformly to fixation process, thus necessitating experimentation with a variety of fixatives and fixatives combinations.

By far the most common strategy for antigen localization is the by the *indirect method*, wherein the antigen is first exposed to an untagged primary antibody. After washing away unbound antibody, a gold particle conjugated-secondary antibody is allowed to bind. Due to the large number of possible combinations of animal species from which the antibodies are derived, the various gold particle sizes and the cost of stocking them, the **Cell Imaging Facility does not provide antibody to be used in the technique.**

It is important to note that antibodies that work well for Western immunoblots do not necessarily work well for immunostaining. Before users proceed to set up an immunogold EM experiment with us, it is often best to try the experiments at the light microscopy level initially. A rough idea of antigen localization can be achieved readily (usually in less than a working day) using light microscopy. Controls may be employed at the light microscopy level to establish the validity of the localization. This is a crucial step, as many of the conditions (fixation, etc.) that optimize localization may be determined with light microscopy. The facility requires users to first perform immunofluorescence with the antibody they want to use for immunogold EM to ensure that the antibody is functional for immunolocalization. Immunofluorescence experiments can be performed here at the facility or in individual labs that have the capacity to do so. Please contact Dr. Wilson Liu and Ms. Satya Khuon to plan for your immunogold EM experiment.

Platinum Replica Electron Microscopy

Conventionally, light and electron microscopy are seldom used in the study of the same biospecimen. Light microscopy allows for dynamic observations of biological processes with great temporal resolution. The spatial resolution of light microscopes, however, is restricted to 200-300 nm. In contrast, electron microscopy allows users to gain very high resolution but only captures a snapshot of static biological structures. Correlative Light and Electron Microscopy (CLEM) thus provides an extremely powerful combination of the advantages of these two techniques to directly link cell structures and dynamics.

The success of CLEM imposes unique demands at light and electron microscopy levels. In order to facilitate the precise identification of corresponding features in EM, users must perform the light microscopy at the highest possible resolution and allow for the fast cessation of dynamic cellular processes at the end of the light microscopic observation.

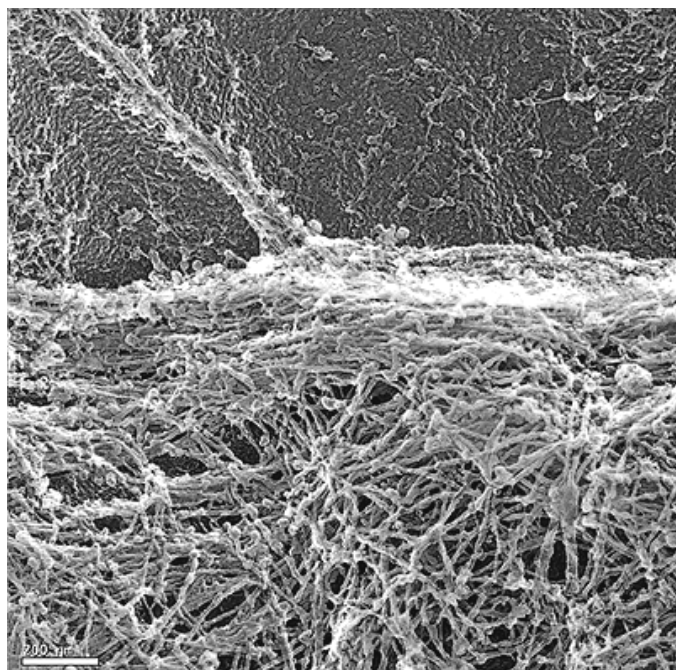


Figure 5 Platinum replica EM of the combined networks of actin and intermediate filament in cultured endothelial cell. An endothelial retraction fiber is clearly at the upper left corner, protruding from the large bundle of cortical actin network.

The Cell Imaging Facility provides the necessary means for users to follow the dynamics of a living cell by time-lapse imaging and subsequently analyze the same cell by EM.

Platinum replica TEM consists of three major steps: (a) detergent extraction, (b) chemical fixation, (b) critical point drying. In the replica EM technique, the contrast is created by shadowing of the three-dimensional samples with metal. The preservation of 3D structures is the major concern during EM processing, especially during drying. The main source of problems is the surface tension at the liquid-gas interface, which will destroy fragile macromolecular structures if the interface passes through the sample. Critical point drying is a simple and reliable technique, which circumvents this problem and preserves the complicated 3D biological structure. See figure 5.

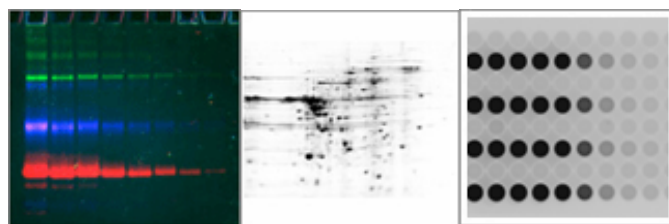
Platinum replica EM can be combined with immunostaining at the EM level. Apparently, CLEM and platinum replica EM are highly involved and complex procedures. Users should expect several rounds of consultation with the facility staff before starting the experiment. Please contact [both](#) Dr. Teng-Leong Chew and Ms. Satya Khuon to set up an initial consultation session to discuss feasibility of this technique for your experiment. We will help you identify the optimal light microscopy instrument and imaging condition, as well as explore the possibility of preserving your structure of interest through the harsh sample processing steps of platinum replica EM.

FujiFilm FLA-5100 Phosphoimager and Fluorescent Scanner

This system, transferred from the former Proteomics Facility with the support of the Robert H. Lurie Comprehensive Cancer Center, is capable of performing advanced fluorescent and radioisotopic detection of protein electrophoresis, and general array analysis.

Large scanning size (up to 40 x 46cm) with selectable scanning area is especially suitable for large size 2D protein electrophoresis gel analysis. Available imaging plates (IPs) include: 1 x (3543 MS IP), 2 x (2340, 2325 MS IP) and 2 x (2040, 2025 MS, SR, ND, TR IP).

The scanning pixel sizes are user-selectable at 10, 25, 50, 100 or 200-micron pixels depending on specific application requirements.



In addition to being a phosphoimager, our FLA-5100 is also equipped with 4 lasers (473nm, 532nm, 635nm, 670nm). This laser combination thus allows users to scan wet gels or membranes as well as scanning multi-well plates.

The FLA-5100 is housed in Morton 2-664. Please contact Dr. Wilson Liu for setting up a user account and training.

Deconvolution

By Brian Northan (pictures by Kevin Ryan)
Media Cybernetics, Inc.

Introduction:

All images taken with a fluorescence microscope suffer from degradation due to noise and blur. Noise is a distortion caused by the quasi random emission and detection of photons. Blur is a distortion caused when light is diffracted as it travels through the limited aperture of the objective lens. Blur can be especially problematic in the axial direction of 3D images made of optical sections. In this article it is assumed that the image can be (and usually is) made of many optical sections in the axial direction. The algorithms described are all developed for this 3D case although most of the algorithms also have a 2D version.

It is important for the microscopist to have a basic understanding of the types of deconvolution algorithms available. Some simple algorithms can actually increase noise and artifacts while more sophisticated deconvolution algorithms will reduce both noise and blur. This article gives an overview of the types of deconvolution algorithms available in AutoQuant. AutoQuant is a suite of deconvolution algorithms available from Media Cybernetics. The main AutoQuant deconvolution algorithm is a highly optimized statistical algorithm based on years of research and development. To show why the advanced statistical algorithm is needed simpler deconvolution algorithms (also available in AutoQuant) are described and compared with AutoQuant's advanced algorithm.

Deconvolution vs. Confocal:

An alternative approach to remove blur is the Confocal microscope. The confocal microscope uses a pin hole to reject out of focus photons. Often people think of deconvolution and confocal microscopy as competing technologies. That is not true. First off since confocal images still contain some blur (especially in the axial direction) deconvolution can still be used to improve image quality. Secondly some specimens cannot survive the higher light exposure used in confocal systems. Wide-field plus deconvolution is the best option for these specimens. Thirdly some situations have characteristics of both confocal and widefield and thus need deconvolution. For example in the case where the confocal pinhole is opened to admit more light or in the case of spinning disk confocal.

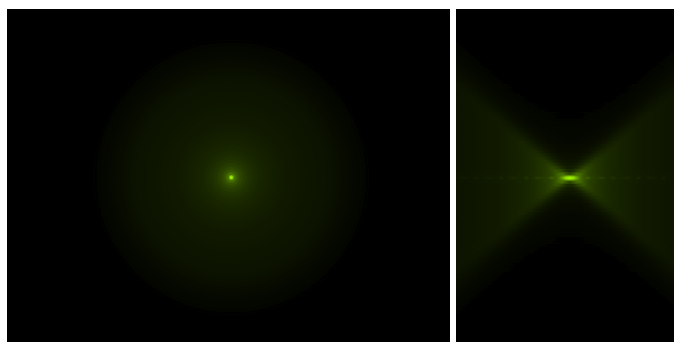


Figure 1 The XY Sum Projection (left) and ZY sum projection (right) of a theoretical PSF assuming an emission wavelength of 550 nm, a numerical aperture of 0.75, and an immersion medium of air.

The PSF and the imaging process:

Fundamental to the understanding of deconvolution is the concept of the PSF. PSF stands for point spread function. The PSF is the fundamental building block of the image. Because of diffraction a point of light at some location of the sample will not look like a point of light in the image. Instead the light will spread out into the pattern which is the PSF. Similarly all points of light in the sample will also look like the PSF and the image will be built from PSF functions not from points. Figure shows a theoretical PSF generated by AutoQuant using diffraction theory. The shape of the PSF is dependent on the modality of the microscope (Widefield, Confocal, etc.) and on the parameters of the imaging system such as the numerical aperture, the emission wavelength, and the refractive index of the immersion medium and sample. The PSF is also affected by aberrations and imperfections if the lenses and other microscope components.

An image is formed by summing the PSFs from each point in the sample where light is emitted. The process of summing all the PSFs is termed convolution. The original sample is said to be convolved with the PSF. Deconvolution is the inverse of convolution. That is deconvolution is used to reverse the effect of convolution with the PSF and restore the true representation of the object.

Object X PSF + noise = observed image

Equation 1 Equation 1 shows a the convolution equation, the observed image is equal to the Object convolved (*) with the PSF plus the noise term. To solve explicitly for the object the PSF function and the noise function needs to be known. Because the noise is random and because the PSF is corrupted by imperfections in the imaging system neither are known precisely.

Overview of deconvolution approaches:

Any solution of the deconvolution equation requires assumptions to be made. To interpret the results of a deconvolution algorithm it is important to understand exactly what assumptions were made when formulating the algorithm. From a high level view AutoQuant supports 3 groups of deconvolution algorithms. The simplest algorithms are a class of essentially ad-hoc algorithms called no/nearest neighbors.

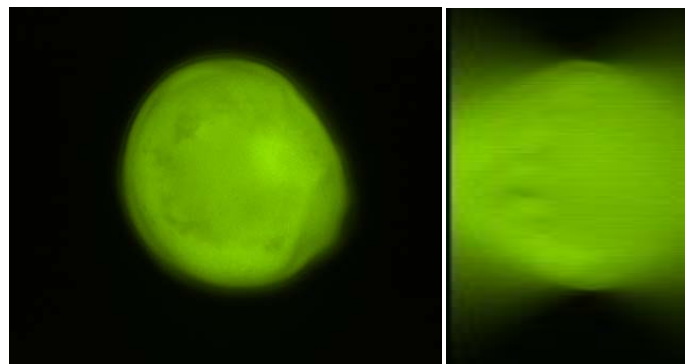


Figure 2 XY (left) and ZY (right) middle slice projection of a pollen grain. To demonstrate the performance of the deconvolution algorithms an image of a pollen grain is used. The image was collected with a 40x 0.75 NA lens. The emission wavelength was 550 nm and the pixel size were x=0.1162, y=0.1162 and z=0.4 microns. The image used is a 432 by 336 ROI that was cropped from a larger image. The image contains 51 optical slices. The middle slice projection of the original image of the pollen grain is shown in Figure . The XY projection is simply the middle (26th) optical section. The ZY view is an axial slice taken at the middle (168th) x position.

A level up in sophistication is the Inverse Filters. These algorithms are designed using the fundamentals of convolution theory. The most sophisticated algorithms belong to a class called constrained iterative algorithms. These are the most sophisticated and accurate algorithms as they include a statistical model of the noise and signal and force realistic constraints. By default choosing the 2D or 3D deconvolution option in the AutoQuant software automatically directs the user to the constrained iterative algorithm. AutoQuant also includes options for the no/nearest neighbors and the inverse filter algorithms. The rest of this article will give a brief overview of these 3 types of deconvolution and explain the advantages and disadvantages of each type.

No/Nearest Neighbors:

The simplest type of deconvolution algorithm that AutoQuant supports are the No and Nearest Neighbors algorithms. These algorithms are fundamentally 2D and work by estimating the blur at a given plane then subtracting the blur from that plane. The blur is estimated by applying a low pass filter to one or more planes adjacent to the plane of interest. In no neighbors the blur function is estimated from the current plane only. In nearest neighbors the blur is estimated from a user-selectable number of surrounding planes. The assumption is that the blur is low frequency and the objects of interest are high frequency. Once the blur is estimated for the current 2D plane it can be removed by subtraction. These algorithms are very fast but they reduce signal levels and can increase noise. Simply subtracting the blur removes signal. A sophisticated algorithm will remove the blur by reallocating instead of eliminating the signal. Simply subtracting the blur can increase the signal to noise ratio because the total signal level will be decreased while high frequency noise remains unchanged. Figure shows the output of the nearest neighbor algorithm when applied to the pollen grain. The haze was estimated from the 2 adjacent planes. Note that while a small amount of detail has been enhanced areas that were hazy in the original image are especially noisy in the output. Unfortunately the haze has been exchanged for noise and the overall image quality is not much better. The nearest neighbor algorithm is fast and can often be found in open source or relatively inexpensive software packages. However the algorithm is simple and often fails because it does not include an underlying model of the system PSF or of the noise.

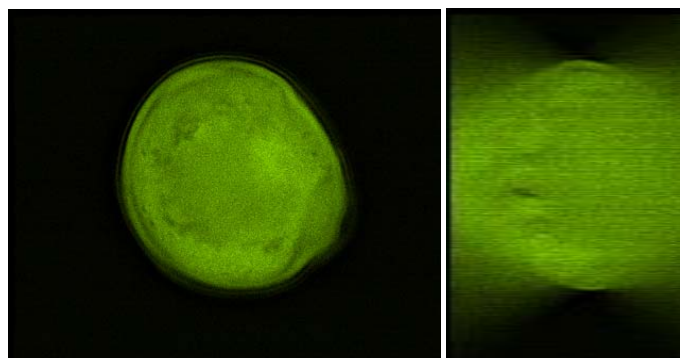


Figure 3 XY (left) and ZY (right) middle slice views of the output of the nearest neighbor algorithm when applied to the pollen grain.

The Inverse Filter:

The inverse filter is a technique that attempts to solve Equation 1 directly. The inverse filter requires that the PSF is known either through measurements of sub-resolution beads or by a theoretical calculation. If noise was not present or the noise was known precisely solving equation 1 would be trivial.

Unfortunately the noise is both present and unknown. This is problematic because if the noise components cannot be removed from the observed image they can be amplified when solving for the object. The solution is to prevent noise amplification by forcing the solution for the object to be relatively smooth. This process is called regularization. Thus the inverse filter is often referred to as a regularized inverse filter. The inverse filter algorithm is fairly fast and tends to produce better results than the no/nearest neighbors methods. Figure shows the output of the inverse filter algorithm when applied to the pollen grain. When compared to Figure more detail can be seen in the XY view and some (but not all) of the blur has been removed in the ZY view. The inverse filter algorithm is prone to artifacts because of the regularization technique used to reduce the noise. Thus the inverse filter algorithm works best in low noise conditions where only a small amount of smoothing is needed. The user interface of many inverse filter implementations (including AutoQuant's) will contain an option for noise level. The result in Figure was obtained using a high noise level. Setting the noise level higher will force the output to be smoother as the algorithm attempts to suppress the noise. In general a result obtained using lower noise settings will contain fewer artifacts from regularization (smoothing). So it is desirable to find an algorithm even more robust against noise. Such an algorithm is described in the next section.

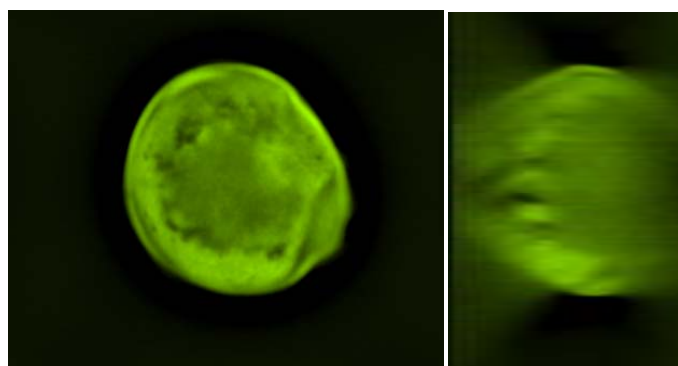


Figure 4 XY (left) and ZY (right) middle slice views of the output of the inverse filter algorithm when applied to the pollen grain.

Constrained Iterative Algorithms:

The most sophisticated deconvolution algorithms belong to a class of algorithms called constrained iterative algorithms. In the general sense a constrained iterative algorithm formulates an estimate for the object, the PSF, and the noise and plugs them into Equation 1 to compute a reconstructed image. The error between the observed image and the reconstructed image is calculated. Then an update rule is used to modify the parameters in such a way that the error is reduced. This process is called optimization. In some algorithms the PSF is not updated but will remain fixed throughout the process. These algorithms are called fixed or non-blind and the PSF is calculated using a theoretical formula or measured using sub-resolution beads. In other algorithms the PSF estimate is allowed to change along with the object. These algorithms are called adaptive PSF or blind algorithms. The adaptive algorithm is convenient because it can be difficult to measure the PSF or calculate it exactly. The imaging system will often have small imperfections such as spherical aberration. Allowing the PSF to vary means the algorithm can adapt to the imaging system. AutoQuant's main deconvolution algorithm is an adaptive PSF algorithm (although a fixed PSF algorithm is also provided).

The noise term in Equation 1 is still unknown. In many constrained iterative algorithms (including AutoQuant's implementation) this is dealt with by modeling the emission and detection of the photons from the object as a random process with Poisson statistics. Starting with this assumption an update rule is derived. When using a constrained iterative algorithm instead of solving the problem all at once the algorithm travels towards the solution.

Thus a stopping criteria needs to be implemented. In AutoQuant the stopping criteria is determined simply by placing a hard limit on the number of iterations. Though there is room for user control as the limit is adjustable. The default setting for the AutoQuant iterative algorithm is 10 iterations. AutoQuant's constrained iterative algorithm has not eliminated the noise but it has achieved a degree of separation of noise and signal (in part) by iteration number. It is important for the user to understand this concept. When running the algorithm for many iterations the user should always inspect the image for signs of noise amplification or other artifacts.

An important part of the constrained iterative algorithm is the constraints. Because the signals are updated iteratively constraints can be applied between iterations. Usually a smoothness constraint is applied to the object to prevent noise amplification. If the adaptive PSF version of the algorithm is being used several constraints are usually applied to the PSF. These constraints force the PSF to be symmetrical and obey the laws of geometrical optics and diffraction theory.

Figure shows the result of 10 iterations of the AutoQuant adaptive PSF constrained algorithm when applied to the pollen grain. Compared to the nearest neighbor's algorithm (Figure) and the inverse filter algorithm (Figure) the constrained iterative algorithm has removed more blur without excessive noise amplification. The noise setting used when running the algorithm was medium (corresponding to a medium amount of smoothing). Recall that when using the inverse filter a high noise level (corresponding to high smoothing) had to be used to generate an acceptable result. This is another major advantage of AutoQuant's constrained iterative approach. It is more robust to noise thus requires less regularization (smoothing) and the output will contain fewer smoothing artifacts that can wipe out detail.

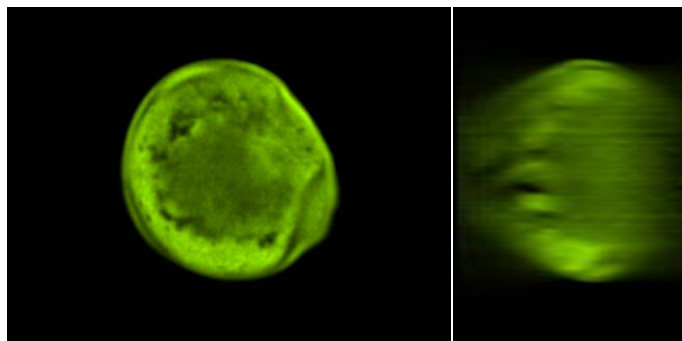


Figure 5 XY (left) and ZY (right) middle slice views of the output of the 10 iterations of the adaptive PSF EM algorithm when applied to the pollen grain.

Conclusions:

In conclusion deconvolution is a fundamentally ill defined problem because Equation 1 has one known, the observed image and three unknowns, the object, the PSF and the noise. Only by making assumptions about the unknowns can a

solution be found. In the nearest neighbors algorithm it is assumed that the blur can be separated from the object by simple linear filtering operations. This is not a good assumption thus nearest neighbors often increases noise and does not optimally reduce blur. In the inverse filter it is assumed that the PSF is known accurately and that the unknown noise can be dealt with by forcing a smoothing criteria on the object. These assumptions are better but still not ideal so the inverse filter usually performs better than nearest neighbors but suffers from noise amplification and artifacts caused by the smoothing criteria. Finally AutoQuant's adaptive PSF constrained iterative algorithm assumes the noise is unknown but follows a Poisson distribution and assumes that the PSF is broadly limited by the laws of optics but can vary within these limits. These assumptions are a good approximation of the true conditions. The AutoQuant algorithm built upon these assumptions has been used in microscopy labs for over 10 years producing high quality deblurred images.

Further Reading/References:

A good overview of deconvolution, comparisons between algorithms, and an depth examination of artifacts.

A Working Person's Guide to Deconvolution in Light Microscopy, Wes Wallace, Lutz H. Schaefer, and Jason R. Swedlow, *BioTechniques* 31:1076-1097 (November 2001).

An in depth mathematical research paper on the algorithm implemented in AutoQuant.

Blind Deconvolution of quantum-limited incoherent imagery: maximum-likelihood approach, Timothy J. Holmes, *Journal of the Optical Society of America*, Vol. 9, No. 7, July 1992.

A good overview of the optics of light microscopy. The first 6 chapters of this book give an excellent overview of the physics of the imaging process. Critical reading to understand how Numerical Aperture, Emission Wavelength, Immersion Medium, Aberrations and other factors affect the shape of the PSF.

Fundamentals of Light Microscopy and Electronic Imaging, Douglas B. Murphy, Copyright 2001 by Wiley-Liss Inc.

© 2008 Northwestern University Cell Imaging Facility

For further information or to obtain training, please contact the following facility staff.

Teng-Leong Chew, Ph.D. 312-503-2841
t-chew@northwestern.edu Morton 2-633

Satya Khuon 312-503-1823
s-khuon@northwestern.edu Morton 2-685

Wilson Liu, M.D. M.Sc. 312-503-1577
Wensheng-liu@northwestern.edu Morton 2-685

Lennell Reynolds, Jr. 312-503-4445
l-reyjr@northwestern.edu Morton 2-672

www.feinberg.northwestern.edu/cif

FEINBERG SCHOOL OF MEDICINE
DEPARTMENT OF CELL & MOLECULAR BIOLOGY



NORTHWESTERN
UNIVERSITY



ROBERT H. LURIE
COMPREHENSIVE CANCER CENTER
OF NORTHWESTERN UNIVERSITY